Contents list available at IJRED website
Int. Journal of Renewable Energy Development (IJRED)
Journal homepage: http://ejournal.undip.ac.id/index.php/ijred

The Effects of Different Roughness Configurations on Aerodynamic Performance of Wind Turbine Airfoil and Blade

Kamyar Jafari[a], Mohammad Hassan Djavareshkian[b,1], Behzad Forouzi Feshalami[b]

[a]*Department of Mechanical Engineering, Eqbal Lahuri Institution of Higher Education, Mashhad, Iran*

[b]*Department of Mechanical Engineering, Ferdowsi University of Mashhad, Iran*

ABSTRACT. In this research, viscous and turbulent flow is simulated numerically on an E387 airfoil as well as on a turbine blade. The main objective of this paper is to investigate various configurations of roughness to find a solution in order to mitigate roughness destructive impacts. Hence, the sand grain roughness is distributed uniformly along pressure side, suction side and both sides during the manufacturing process. Navier-Stokes equations are discretized by the finite volume method and are solved by SIMPLE algorithm in the OpenFOAM software which is open source. Results indicated that in contrast with previous studies, the roughness will be useful if it is applied on only pressure side of the airfoil. In this condition, the lift coefficient is increased to 8.62% and 1.2% compare to the airfoil with rough and smooth sides, respectively. However, in 3-D simulation, the lift coefficient of the blade with pressure surface roughness is less than smooth blade, but still its destructive impacts are much less than of both surfaces roughness and suction surface roughness. Therefore, it can be deduced that in order to reveal the influence of roughness, the simulation must be accomplished in three dimensions.

Keywords: Roughness, wind turbine blade, aerodynamic, E387 airfoil, CFD

Article History: Received Jun 12th 2017; Received in revised form August 27th 2017; Accepted Oct 3rd 2017; Available online
How to Cite This Article: Jafari, K., Djavareshkian, M.H., Feshalami, B.H. (2017) The Effects of Different Roughness Configurations on Aerodynamic Performance of Wind Turbine Airfoil and Blade. International Journal of Renewable Energy Develeopment, 6(3), 273-281.
https://doi.org/10.14710/ijred.6.3.273-281

1. Introduction

Wind energy, which is one of the renewable sources, has been significantly developed in recent years. At the end of 2015, the wind turbine installed capacity is reached 63,467 MW (Globalwindstatistics. et al.). Surface roughness is one of the critical factors to pull aerodynamic performance of wind turbine down. Roughness can be considered as obstacles which are settled into the viscous layer. These obstacles increase interaction between fluid and solid. Consequently, it can seriously affect the aerodynamic performance of airfoil (Sagol, Reggio, & Ilinca 2013). Chakroun, Al-Mesri, & Al-Fahad (2004) highlighted that stall angle can be delayed when the surface is rough. Also, when the roughness is located at trailing edge, it has the least adverse impact on performance. Darbandi et al. (2014) showed that annual energy production is faced with a 25% reduction when roughness is exerted on wind turbine blade. By performing experimental and numerical research on a NACA63-618 airfoil, Walker et al. (2014) revealed that roughness reduces the maximum power coefficient to 0.34 while this coefficient is 0.42 for clean one.

Effects of roughness height have been investigated by many researchers. Wu, Li, & Li (2013) showed that the performance of a wind turbine airfoil is very sensitive to the roughness height of $0.6\,mm$. Also, $53\% - 92\%$ of suction surface and $44\% - 88\%$ of pressure surface are the most sensitive regions. Soltani, Askari, & Sadri (2016) experimentally revealed that aerodynamic efficiency is reduced and the drag is increased for airfoil with roughness height of

[1] Corresponding author: javareshkian@um.ac.ir

0.5 mm. By performing experimental research, David et al. (2016) studied the effects of roughness on the performance of NACA63-415 and SERIS814 airfoils. Results indicated that increment of roughness height has more influence on SERIS814 airfoil in order to reduce maximum lift and lift to drag ratio than the NACA63-415 airfoil. Bai et al. (2014) numerically pointed out that the total pressure loss coefficient is reached 129% for the rough blade in comparison with the smooth blade. Also, Re enhancement has unfavorable effects on the performance of the rough blade. By performing experimental research on a 53° leading edge sweep diamond wing, Hövelmann, Knoth, & Breitsamter (2016) showed that roughness height significantly affects the flow separation onset and the emerging leading edge vortex. Khanjari, Sarreshtehdari, & Mahmoodi (2017) concluded that increment of roughness height from 0 to 0.5 mm reduces the net power.

Environmental conditions, including dusty, rainy and snowy weathers, can jeopardize aerodynamic performance of wind turbine due to the increment of the blade roughness (Zidane et al. 2016). Effects of various Re, roughness height and roughness shape in a dusty condition experimentally tested by Hummel et al. (2005). They showed that increment of Re increases total pressure losses. They also revealed that at $Re = 1.2 \times 10^6$ and the surface roughness height of 11.8 μm, total pressure loss is faced with 40% enhancement in comparison with the smooth surface. Influence of dust accumulation on performance of wind turbine experimentally examined by Khalfallah & Koliub (2007). They showed that by enhancement of dust on wind turbine blades, drag increases while lift reduces. This can finally lead to reduction of power production. They also mentioned that this reduction depends on airfoil type, Re, sand size based on boundary layer thickness and nature of roughness. Homola et al. (2010) numerically analyzed impacts of temperature and droplet size on the aerodynamic performance of a wind turbine blade. They expressed that the temperature and droplet size don't have significant effect on flow separation of the blade at 5° angle of attack. However, by increasing the angle of attack to 15°, reduction of temperature and enhancement of droplet size, respectively, reduces and increases flow separation. By simulating a NACA0012 airfoil under heavy rain condition, Douvi & Margaris (2012) proved that rain drop increases drag and also leads to lift reduction. They also showed that this variation can be intensive at higher Re and angle of attack. El-Din & Diab (2016) numerically investigated behavior of various airfoils against created roughness by erosion of sands. They showed that NREL airfoils have higher resistance to erosion than the other types, namely NACA and DU, at higher angle of attack.

There are lots of numerical methods to investigate the impacts of roughness on flow behavior. Meng-Huang & William (2009) examined ability of a new second-order closure of the rough wall layer model in order to simulate a rough NACA0012 airfoil. Results showed that this method can properly predict the aerodynamic characteristics of flow before separation. Capability of two models, low Reynolds number shear stress transport model and $\gamma - R_\theta$ shear stress transport model, to simulate a rough NACA0012 airfoil is studied by Liu & Qin (2014). Results indicated that first method is able to simulate the roughness of surface properly while the other model is not. CFD methods have been widely used to evaluate aerodynamic performance of wind turbine. Munduate & Ferrer (2009) evaluated the capability of panel method and CFD technique in order to predict wind turbine blade life cycle under different conditions. Results revealed that panel method is not reliable to simulate roughness effects of fully turbulent flows. In contrast, obtained results by CFD methods have been had acceptable agreement with experimental data.

Performance of Wind turbine blade is sensitive to roughness patterns. Timmer & Schaffarczyk (2004) experimentally showed that the adverse impacts of carborundum 60 roughness are more than of zigzag tape roughness on performance of a DU97-w-300 airfoil. However, increasing Re mitigates these undesirable impacts. Soltani, Birjandi, & Seddighi Moorani (2011) experimentally proved that zigzag and strip tape roughness patterns have less effect on flow characteristics than that of distributed contamination. To summarize, all of the studies have been revealed that existence of roughness for any reason decreases the aerodynamic efficiency. Furthermore, increasing angle of attack and roughness height can also intensify roughness adverse impacts. It was also shown that the results are very sensitive to the roughness pattern. The main objective of this paper is to investigate effects of various roughness configurations on wind turbine aerodynamic performance. Hence, E387 airfoil and blade, which can be used in wind turbines, are considered to do simulations (Krishnaswami 2013). The sand grain roughness is distributed uniformly along pressure side, suction side and both sides during manufacture process. The authors aimed to find the solution in order to mitigate the disadvantages of roughness on the performance of a wind turbine. Moreover, simulations are conducted in two and three dimensions to reveal why the results in two dimensions may lead to an egregious inaccuracy.

2. Numerical method

2.1. Governing equations and discretization

Conservation laws, namely continuity and momentum, are governing equations which are represented as follows:

$$\frac{\partial \rho}{\partial t} + \nabla . \rho V = 0 \quad (1)$$

$$\frac{\partial}{\partial t}(\rho u_i) + \frac{\partial}{\partial x_j}(\rho u_i u_j) = -\frac{\partial P}{\partial x_i} + \frac{\partial \tau_{ij}}{\partial x_j} + F_i \quad (2)$$

where ρ and V are density and velocity vector of fluid. u_i and u_j are velocity in x and y directions. Also, P, τ_{ij} and F_i show, respectively, pressure, stress tensor and internal force.

Stress tensor can be expressed by:

$$\tau_{ij} = \left[\mu\left(\frac{\partial u_i}{\partial x_j} + \frac{\partial u_j}{\partial x_i}\right)\right] \quad (3)$$

$$\frac{\partial}{\partial t}(\rho k) + \frac{\partial}{\partial x_i}(\rho k u_i) = \frac{\partial}{\partial x_j}\left(\Gamma_k \frac{\partial k}{\partial x_j}\right) + \tilde{G}_k - Y_k + S_k \quad (4)$$

$$\frac{\partial}{\partial t}(\rho \omega) + \frac{\partial}{\partial x_i}(\rho \omega u_i) = \frac{\partial}{\partial x_j}\left(\Gamma_\omega \frac{\partial \omega}{\partial x_j}\right) + \tilde{G}_\omega - Y_\omega + D_\omega + S_\omega \quad (5)$$

where μ is viscosity. To simulate turbulence effects, $SST\ k-w$ model is applied in these equations, where k and ω indicate turbulent kinetic energy and energy loss rate. Also $Y, D, S, \tilde{G}$ and Γ are terms of loss, propagation length, source, production rate and diffusion, respectively

Wall function law, which is shown in eq. (6), is modified for rough walls in eq. (7) (Ioselevich & Pilipenko 1974):

$$u^+ = \frac{1}{K} ln(y^+) + B \quad (6)$$

$$\frac{u_p u^*}{\tau_\omega / \rho} = \frac{1}{k} ln\left(E \frac{\rho u^* y_p}{\mu}\right) - \Delta B \quad (7)$$

$$u^* = c_\mu^{1/4} k^{1/2} \quad (8)$$

where k is Von Karman constant and is equal to 0.04. u_p is the center velocity of first cell near surface and y_p indicates the distance between point p and rough wall. c_μ is experimental constant and is equal to 0.09. Also, ΔB is the roughness function and is related to roughness types, including uniform sand, rivets, threads ribs, mesh-wire and etc., and roughness size. It should be noted that there is not general roughness function valid for all roughness types. Roughness function is related to normalized roughness average height that is shown by k^+. This parameter can be calculated as follows:

$$K_s^+ = \frac{\rho R_a u^*}{\mu} \quad (9)$$

where k is the turbulent kinetic energy of the cells that is located near the wall. In this paper, the Arithmetic Average Height, R_a, is used to express roughness parameter (Gadelmawla et al. 2002). This can be defined as follows:

$$R_a = \frac{1}{n}\sum_{i=1}^{n}|y_i| \quad (10)$$

where y_i indicates heights of roughness. According to this equation, R_a is average absolute deviation of roughness oscillations. In this research, various values of R_a are examined to show its effects on aerodynamic performance.

There are three distinct regimes for rough wall: (1) smooth regime with $K_s^+ < 3\sim5$ (2) transient regime with $3\sim5 < K_s^+ < 70\sim90$ and (3) fully rough regime with $K_s^+ > 70\sim90$ (Cebeci & Bradshaw 1977). Values of roughness function for transition and fully rough regimes can be acquired by eqs. (11) and (12), respectively: C_s is the roughness coefficient and depends on the type of roughness. In this research, content of 0.5 is considered for uniform sand grain roughness and more values can be used for non-uniform one (Levin, Semin, &Klyukin 2014). Eqs. (11) and (12) are used for sand grain roughness and similar types of uniform roughness elements. Navier-Stokes equations are discretized by the finite volume method and are solved by the SIMPLE implicit method.

$$\Delta B = \frac{1}{k}\ln\left(\frac{K_s^+ - 2.25}{87.75} + C_s K_s^+\right) \times \sin\{0.4258(\ln K_s^+ - 0.811)\} \quad (11)$$

$$\Delta B = \frac{1}{k}\ln(1 + C_s K_s^+) \quad (12)$$

2.2. Mesh and boundary condition

In order to produce proper mesh, center height of first cell in the vicinity of the wall must be equal or more than of roughness average height. It should be noted that roughness effect cannot be observed in the simulation process when the height of first cell is considered much more than of roughness average height (Natarajan & Hangan 2009). Logarithmic region is suitable for computational domain to evaluate roughness effect. Thus, Y^+ is restricted between 30 and 500 (Blocken, Stathopoulos, &Carmeliet 2007). Contents of $10c$ and $25c$ are considered as width and length of computational domain of airfoil, which is shown in Fig. 1.

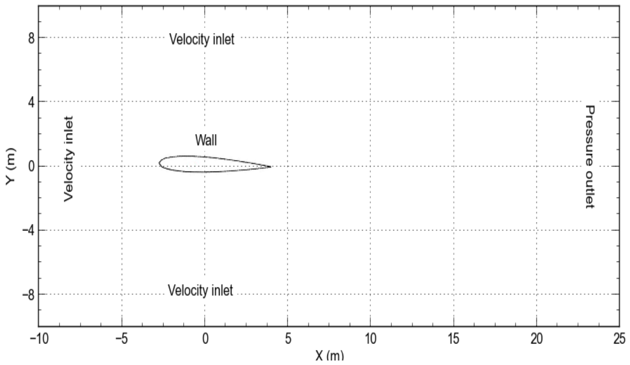

Fig. 1. Computational region and boundary conditions for airfoil

As demonstrated in Fig. 2, the mesh is as structured type. On the other hand, unstructured mesh is used for wind turbine blade due to the complexity of geometry. Computational domain and Periodic boundary condition are shown in Fig. 3 for wind turbine blade with radius of 17 m.

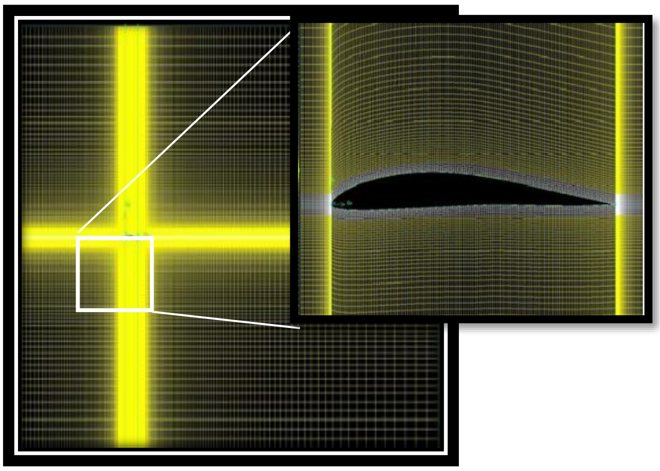

Fig. 2. Mesh around E387 airfoil

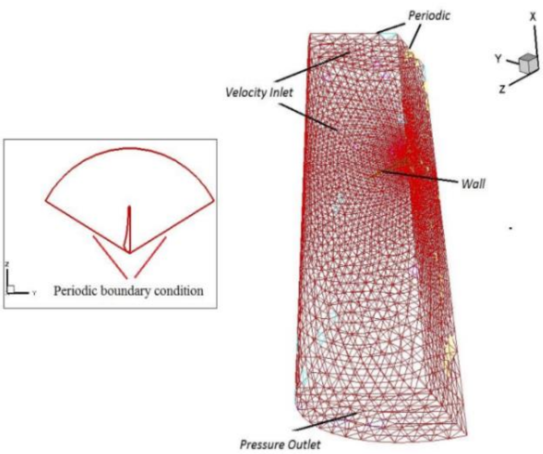

Fig. 3. Computational region and boundary conditions around wind turbine blade

2.3. Mesh independency and validation

For airfoil simulation, mesh with cell numbers of 78,000, 106,000 and 159,200 are generated to investigate mesh independency. Pressure coefficient, C_p, for aforementioned meshes are illustrated in Fig. 4 $at\ Re = 4.6 \times 10^5$ and $0°$ angle of attack. Moreover, Grid solution study for turbine blade has been performed to ensure independency of the results from the mesh. Hence, C_p at $0.95c$, wind velocity of 20 $^m/_s$ and angular velocity of 6.17 $^{rad}/_s$ are depicted in Fig. 5 for various cell numbers. According to these figures, by increasing mesh cell numbers from 106,000 to 152,200 for the airfoil and from 1,029,597 to 1,467,876 for the blade, although computational cost increases, the accuracy is almost constant. Therefore, the meshes with cell numbers of 106,000 and 1,029,597 are employed for the airfoil and blade, respectively.

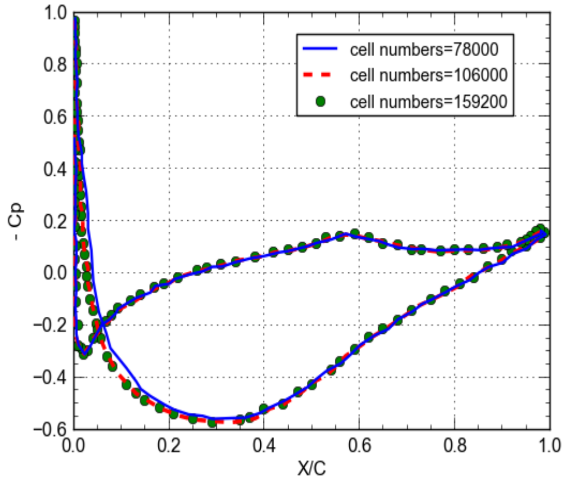

Fig. 4. Mesh independency based on pressure coefficient distribution for the E387 airfoil at $\alpha = 0$

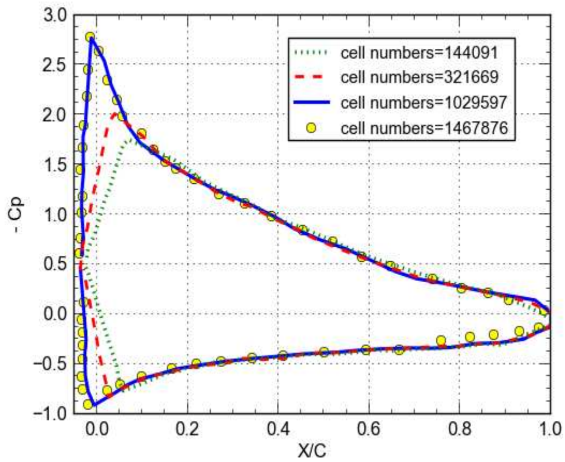

Fig. 5. Mesh independency based on pressure coefficient distribution at 95% of blade radius

Due to the lack of experimental research about present airfoil, firstly simulation is conducted on a S809 airfoil and is compared with experimental data of Somers (1989) in Fig. 6. Then, lift coefficient of present research for the E387 airfoil is compared with that of Bidarouni & Djavareshkian (2013) in Fig. 7 at $Re = 4.6 \times 10^5$, 0, 5 and 10° angles of attack, $\rho = 1.225\ {}^{kg}/_{m^3}$ and $\mu = 1.7894$. It should be noted that in this figure, $k - \varepsilon$ turbulence model is used to compare with that of Bidarouni & Djavareshkian (2013) in order to prove trueness of present simulation. However, this model doesn't have acceptable performance in high angles of attack due to generation of reversible flows. Therefore, $SST\ k - w$ model is applied to do simulations(Versteeg & Malalasekera 2007). Also, power coefficient of current study is compared with that of Saber & Djavareshkian (2014) in Fig. 8 for various wind velocities. Additionally, In order to prove trueness of roughness simulation, lift coefficient of a NACA630-430 airfoil at $\rho = 1.225\ {}^{kg}/_{m^3}$, $\mu = 1.7894\ {}^{kg}/_{m.s}$, $Re = 1.6 \times 10^6$ and $R_a = 0.5, 1\ mm$ is compared with data of Ren & Ou (2009). The difference in results, which are tabulated in Table 1, can be justified as discrepancy of two studies in mesh generation.

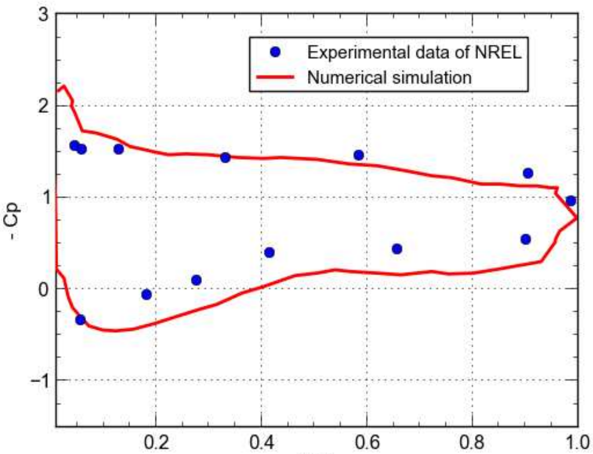

Fig. 6. Comparison of pressure coefficient distribution between present study and experimental data of Somers (1989) at 50% of the S809 blade

Table 1.
Comparison of the lift coefficient of present simulation with that of Ren and Ou (Ren & Ou 2009) for the NACA630-430 airfoil

R_a (mm)	Lift coefficient of Ren & Ou (2009)	Lift coefficient of present simulation
0.5	0.48	0.44
1	0.46	0.41

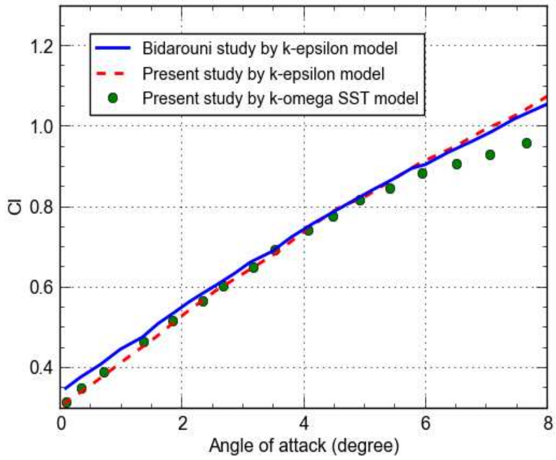

Fig. 7. Comparison of present simulation with numerical results of Bidarouni & Djavareshkian (2013) for E387 airfoil

3. Results and discussion

Firstly, the airfoil with different roughness average heights of 0, 0.06, 0.1, 0.3, 0.5, 0.8 and 1 mm is simulated numerically at $Re = 1.6 \times 10^6$ and $\alpha = 5°$. It should be noted that the simulation is accomplished at first on the smooth airfoil and then the mentioned roughness average heights are exerted to both sides of the airfoil. As demonstrated in Figs. 9 and 10, by increment of roughness average height, lift coefficient diminishes while the drag increases. But after a specific height, there is not a significant alteration in these coefficients.

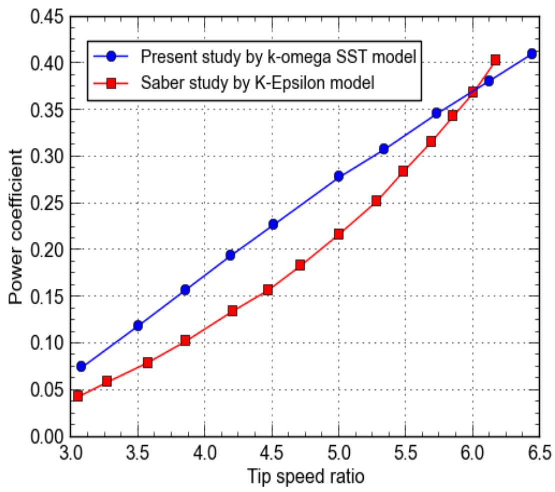

Fig. 8. Comparison of present simulation with numerical results of Saber & Djavareshkian (2014) for blade

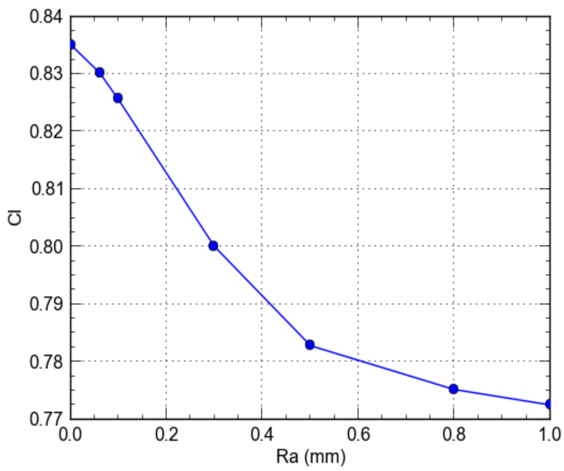

Fig. 9. Lift coefficient for various roughness average heights at $\alpha = 5°$

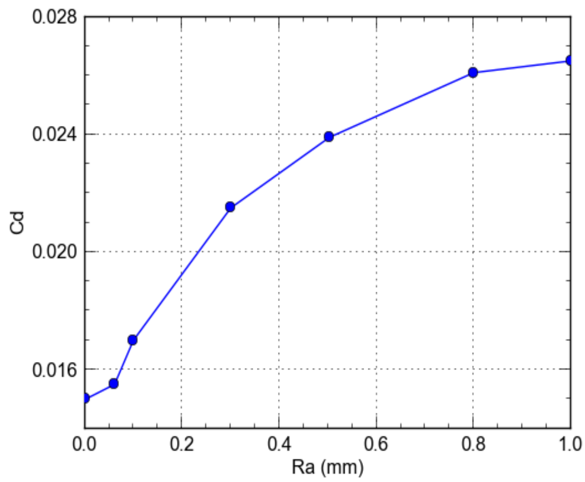

Fig.10. Drag coefficient for various roughness average heights at $\alpha = 5°$

As listed in Table 2, Reduction in pressure difference can justify decrement of aerodynamic efficiency. However, based on Table 3, it is observed that adding the roughness to one side of the airfoil can lead to different results. In the other words, by exerting roughness to only pressure side, lift force is faced with 8.62% enhancement in comparison with the airfoil with rough sides. Also, there is an 1.2% improvement in lift coefficient in comparison with the airfoil with smooth sides because as demonstrated in Figs. 11 and 12, the roughness reduces the flow velocity in the vicinity of the pressure side. Therefore, the positive pressure difference is increased much more than of other conditions. In addition, roughness not only doesn't have destructive impacts but also increases aerodynamic performance.

Table 2.
Lift and drag coefficients of airfoil with both sides roughness at $\alpha = 5°$ and $R_a = 0, 0.8\,mm$

R_a (mm)	Lift (N)	Drag (N)
0	352.89	6.37
0.8	328.29	11.04

In contrast, roughness on only suction side has adverse impacts. Because in this condition, roughness is the factor to increase boundary layer thickness and leads to movement of the separation point toward the leading edge (see Fig. 13). Moreover, based on Figs. 11 and 12, roughness plays an important role to change aerodynamic and pressure coefficients when it is exerted to $0.6c$ of airfoil from leading edge. However, by reaching the trailing edge, impacts of roughness are negligible because this region is located within the turbulent flow. Additionally, the pressure difference between upper and lower sides at leading edge is increased than the other locations.

To investigate the validity of mentioned configurations on turbine blade, the roughness with average heights of $0, 0.1, 0.2$ and $0.3\,mm$ are applied on surfaces of the turbine blade. Output torque of rough blade is less than of smooth blade. Therefore, it causes a reduction of energy production (Table 4 and Fig. 14). Energy production of wind turbine is generally increased by increment of tip speed ratio of the blade. Based on Fig. 15, when roughness is added to this blade, energy production will be reduced in comparison with smooth blade because in the rough blade, the possibility of separation increases by enhancement of wind velocity and subsequently the flow will be less in touch with blade surface.

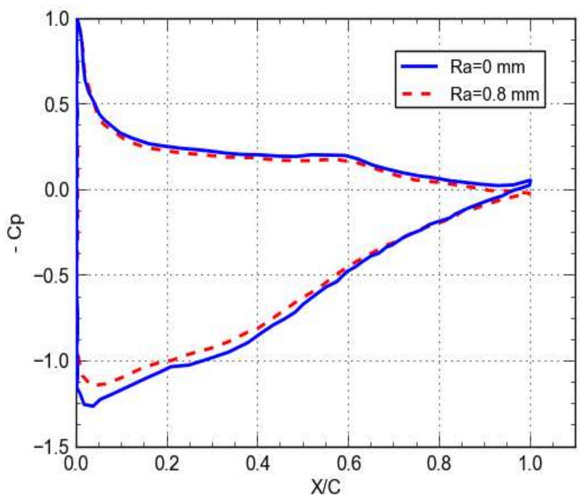

Fig. 11. Pressure coefficient distribution along the airfoil sides for different roughness average heights at $\alpha = 5°$

Table 3.
Lift and drag coefficients for different roughness configurations of airfoil at $\alpha = 5°$ and $R_a = 0.8\ mm$

R_a (mm)	Output torque (N-m)	Reduction percentage of output torque (%)
0	60953.37	-
0.1	58013.07	4.82
0.2	56650.36	7.05
0.3	55710.48	8.60

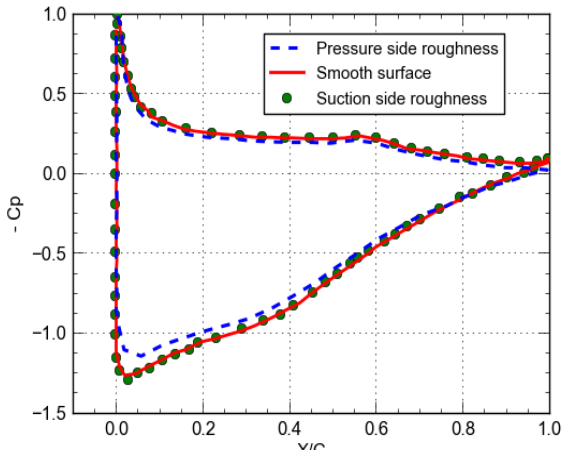

Fig. 12. Distribution of pressure coefficient along airfoil sides for three roughness configurations at $\alpha = 5°$ and $R_a = 0.8\ mm$

As illustrated in Fig. 16, in contrast with airfoil, the lift force of blade with only pressure surface roughness is less than of blade with smooth surfaces. Nevertheless, roughness on the only pressure surface of the blade has less energy production reduction than suction surface and still can be better solution than the blade with rough surfaces. This is that reason which leads to difference between two and three dimensional simulations.

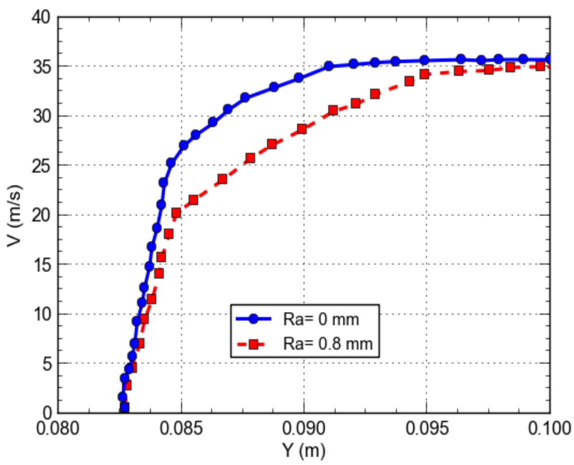

Fig. 13. Boundary layer thickness for suction side of airfoil at $x/c = 0.35$, $R_a = 0,8\ mm$ and $\alpha = 5°$

Table 4.
Output torque of turbine blade for different Roughness average heights

Roughness Configuration	Lift Coefficient	Lift force (N)
Smooth	0.83	351.96
Suction side	0.77	324.76
Pressure side	0.84	356.62

Two dimensional simulation of Roughness on the only pressure side increased the lift force more than of airfoil with smooth sides while adverse results are obtained in three dimensional simulation. Because separation point on wind turbine blade at each radius is different due to the existence of pitching angle. Therefore, it can be concluded that in order to achieve accurate results, the simulations must be accomplished in three dimensions.

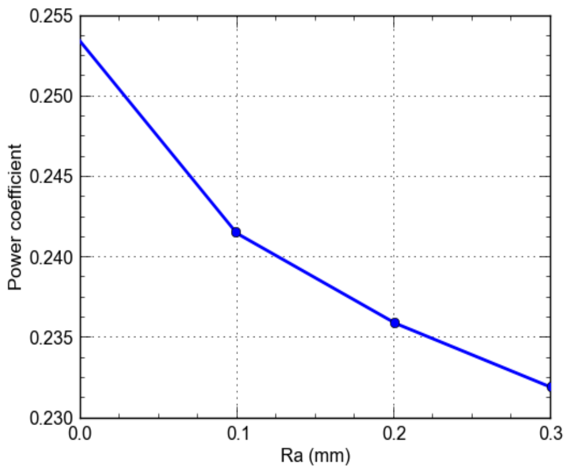

Fig. 14. Variations of turbine Power coefficient versus roughness average height at wind speed of 20 m/s

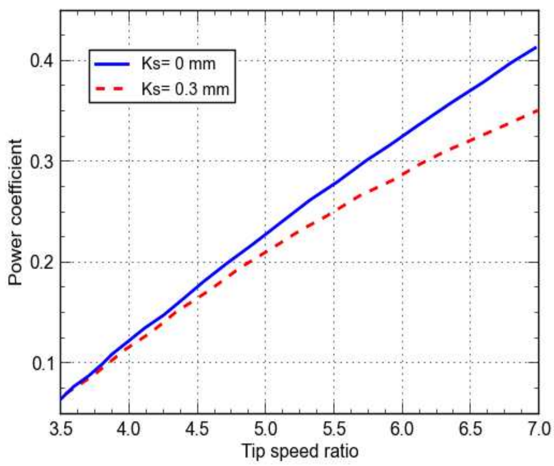

Fig. 15. Variations of turbine power coefficient for various tip speed ratio at $R_a = 0, 0.3\ mm$

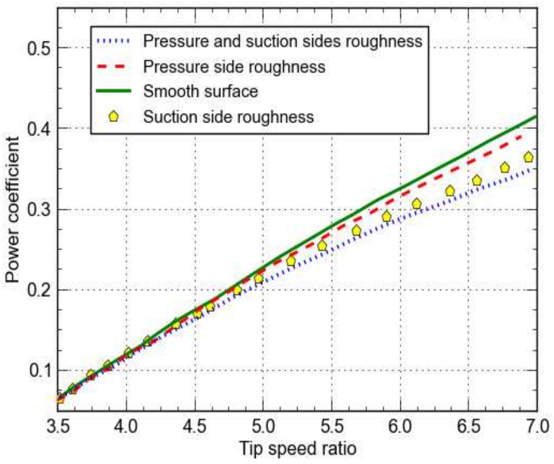

Fig. 16. Variations of turbine power coefficient for various roughness configurations and $R_a = 0.3\ mm$

4. Conclusion

Various roughness configurations were simulated numerically on an E387 airfoil and blade. The main objective of this paper was to choose the best configuration in order to mitigate destructive impacts of roughness. Navier-Stokes equations were discretized by the finite volume method and were solved by SIMPLE algorithm. The main findings of present study can be summarized as follows:

- When roughness is added to the only pressure side of the airfoil, the lift force faced with 8.62% enhancement in comparison with the airfoil with rough sides. However, the lift force of blade with only pressure surface roughness is less than of smooth surface. Nevertheless, roughness on the only pressure surface of the blade has less energy production reduction than suction surface and still can be a better solution than the blade with rough surfaces.
- By applying the roughness on the only suction side of the airfoil, lift and drag are, respectively, reduced and increased due to the increment of boundary layer thickness and movement of transient point toward the airfoil leading edge.
- Output power is reduced by applying roughness on turbine blades.
- Roughness plays an important role to change aerodynamic and pressure coefficients when it is exerted to 0.6c of airfoil from the leading edge. However, by reaching the trailing edge, impacts of roughness are negligible because this region is located within the turbulent flow.
- There is no alteration in aerodynamic performance higher than of critical roughness average height.

References

Bai, T., Liu, J., Zhang, W., & Zou, Z. (2014). Effect of surface roughness on the aerodynamic performance of turbine blade cascade. Propulsion and Power Research, 3(2), 82-89.

Bidarouni, A. L., & Djavareshkian, M. H. (2013). An Optimization of Wind Turbine Airfoil Possessing Good Stall Characteristics by Genetic Algorithm Utilizing CFD and Neural Network. International Journal Of Renewable Energy Research, 3(4), 993-1003

Blocken, B., Stathopoulos, T., & Carmeliet, J. (2007). CFD simulation of the atmospheric boundary layer: wall function problems. Atmospheric environment, 41(2), 238-252.

Cebeci, T., & Bradshaw, P. (1977). Momentum transfer in boundary layers. Washington, DC, Hemisphere Publishing Corp.; New York, McGraw-Hill Book Co., 1977. 407

Chakroun, W., Al-Mesri, I., & Al-Fahad, S. (2004). Effect of surface roughness on the aerodynamic characteristics of a symmetrical airfoil. Wind Engineering, 28(5), 547-564.

Darbandi, M., Mohajer, A., Behrouzifar, A., Jalali, R., & Schneider, G. E. (2014). Evaluating the effect of blade surface roughness in megawatt wind turbine performance using analytical and numerical approaches. 10th International Conference on Heat Transfer, Fluid Mechanics and Thermodynamics Florida.

David, C. M., Edward, B. W., Benjamin, W., Christopher, M. L., Dam, C. P. v., & Joshua, A. P. (2016). Experimental Measurement and CFD Model Development of Thick Wind Turbine Airfoils with Leading Edge Erosion. Journal of Physics: Conference Series, 753(2).

Douvi, E., & Margaris, D. (2012). Aerodynamic Performance Investigation under the Influence of Heavy Rain of a NACA 0012 Airfoil for Wind Turbine Applications. International Review of Mechanical Engineering (I. RE. ME), 6(6), 1228-1235.

El-Din, A. H., & Diab, A. (2016). A Preliminary Study of the Blade Erosion for a Wind Turbine Operating in a Dusty Environment. ASME Turbo Expo : Turbomachinery Technical Conference and Exposition.

Gadelmawla, E. S., Koura, M. M., Maksoud, T. M. A., Elewa, I. M., & Soliman, H. H. (2002). Roughness parameters. Journal of Materials Processing Technology, 123(1), 133-145.

GlobalWindEnergyCouncil(GWEC).Globalwindstatistics., http://www.gwec.net/wp-content/up-, A. f., loads/vip/GWEC-Global-Wind-2015-Report_April-2016_, & 22_04.pdf.) Accessed on April 27,

Homola, M. C., Virk, M. S., Wallenius, T., Nicklasson, P. J., & Sundsbø, P. A. (2010). Effect of atmospheric temperature and droplet size variation on ice accretion of wind turbine blades. Journal of Wind Engineering and Industrial Aerodynamics, 98(12), 724-729

Hövelmann, A., Knoth, F., & Breitsamter, C. (2016). AVT-183 diamond wing flow field characteristics Part 1: Varying leading-edge roughness and the effects on flow separation onset. Aerospace Science and Technology, 57, 18-30.

Hummel, F., Lötzerich, M., Cardamone, P., & Fottner, L. (2005). Surface roughness effects on turbine blade aerodynamics. Journal of Turbomachinery, 127(3), 453-461.

Ioselevich, V., & Pilipenko, V. (1974). Logarithmic velocity profile for flow of a weak polymer solution near a rough surface. Soviet Physics Doklady.

Khalfallah, M. G., & Koliub, A. M. (2007). Effect of dust on the performance of wind turbines. Desalination, 209(1), 209-220.

Khanjari, A., Sarreshtehdari, A., & Mahmoodi, E. (2017). Modeling of Energy and Exergy Efficiencies of a Wind Turbine Based on the Blade Element Momentum Theory

Under Different Roughness Intensities. Journal of Energy Resources Technology, 139(2), 022006.https://energyresources.asmedigitalcollection.asme.org/article.aspx?articleID=2552721

Krishnaswami (2013). Experimental Analysis of Near and Transitional Wind Turbine Wake Using Stereo Particle Image Velocimetry. Master of Science Thesis, Delft University of Technology.

Levin, L. Y., Semin, M. A., & Klyukin, Y. A. (2014). Estimation of wall roughness functions acceptability in CFD simulation of mine ventilation networks. Proceedings of Summer School-Conference "Advanced Problems in Mechanics

Liu, S., & Qin, N. (2014). Modelling roughness effects for transitional low Reynolds number aerofoil flows. Proceedings of the Institution of Mechanical Engineers, Part G: Journal of Aerospace Engineering, 229(2), 280-289.

Meng-Huang, L., & William, W. L. (2009). Numerical Study of Roughness Effects on a NACA 0012 Airfoil Using a New Second-Order Closure of the Rough Wall Layer Modeling. 47th AIAA Aerospace Sciences Meeting including The New Horizons Forum and Aerospace Exposition.https://arc.aiaa.org/doi/abs/10.2514/6.2009-52

Munduate, X., & Ferrer, E. (2009). CFD Predictions of Transition and Distributed Roughness Over a Wind Turbine Airfoil. 47th AIAA Aerospace Sciences Meeting including The New Horizons Forum and Aerospace Exposition.http://dx.doi.org/10.2514/6.2009-269

Natarajan, D., & Hangan, H. (2009). Numerical study on the effects of surface roughness on tornado-like flows. 11th Americas Conference on Wind Engineering

Ren, N., & Ou, J. (2009). Dust effect on the performance of wind turbine airfoils. Journal of Electromagnetic Analysis and Applications, 1(2), 102

Saber, M. R., & Djavareshkian, M. H. (2014). Comparison of Performance Base and Optimized Blades of Horizontal Axis Wind Turbine. International Journal of Renewable Energy Research (IJRER), 4(1), 61-68

Sagol, E., Reggio, M., & Ilinca, A. (2013). Issues concerning roughness on wind turbine blades. Renewable and Sustainable Energy Reviews, 23, 514-525.

Soltani, M., Askari, F., & Sadri, V. (2016). Roughness and turbulence effects on the aerodynamic efficiency of a wind turbine blade section. Scientia Iranica. Transaction B, Mechanical Engineering, 23(3), 927-941.https://search.proquest.com/openview/57f8fb491dc14cc794885c351d39ae78/1?pq-origsite=gscholar&cbl=54701

Soltani, M. R., Birjandi, A. H., & Seddighi Moorani, M. (2011). Effect of surface contamination on the performance of a section of a wind turbine blade. Scientia Iranica, 18(3), 349-357.

Somers, D. M. (1989). "Design and Experimental Results for the S809 Airfoil." from http://www.nrel.gov/docs/legosti/old/6918.pdf.

Timmer, W., & Schaffarczyk, A. (2004). The effect of roughness at high Reynolds numbers on the performance of aerofoil DU 97-W-300Mod. Wind Energy, 7(4), 295-307.

Versteeg, H. K., & Malalasekera, W. (2007). An introduction to computational fluid dynamics: the finite volume method, Pearson Education.

Walker, J. M., Flack, K. A., Lust, E. E., Schultz, M. P., & Luznik, L. (2014). Experimental and numerical studies of blade roughness and fouling on marine current turbine performance. Renewable Energy, 66, 257-267.

Wu, P., Li, C., & Li, Z. M. (2013). Numerical Simulation of Influence with Surface Contamination on Aerodynamic Performance of Dedicated Wind Turbine Airfoil. Advanced Materials Research, 724, 572-575.

Zidane, I. F., Saqr, K. M., Swadener, G., Ma, X., & Shehadeh, M. F. (2016). On the role of surface roughness in the aerodynamic performance and energy conversion of horizontal wind turbine blades: a review. International Journal of Energy Research, 40(15), 2054–2077